Numerical experiments on one-dimensional model of turbulence

J. Qian[a)]
Institute of Mechanics, Chinese Academy of Sciences, Beijing, The People's Republic of China and Department of Mechanical Engineering, The City College of the City University of New York, New York 10031

(Received 9 June 1983; accepted 7 February 1984)

The initial-value problem of a forced Burgers equation is numerically solved by the Fourier expansion method. It is found that its solutions finally reach a steady state of "laminar flow" which has no randomness and is stable to disturbances. Hence, strictly speaking, the so-called Burgers turbulence is not a turbulence. A new one-dimensional model is proposed to simulate the Navier–Stokes turbulence. A series of numerical experiments on this one-dimensional turbulence is made and is successful in obtaining Kolmogorov's $k^{-5/3}$ inertial-range spectrum. The (one-dimensional) Kolmogorov constant ranges from 0.5 to 0.65.

I. INTRODUCTION

The difficulties of the problem of turbulence are twofold: in part they are connected with the complicated vectorial character of the Navier–Stokes equation; in part they are dependent upon the presence of nonlinear terms. The latter feature is essential for turbulence; a linear dynamic system cannot generate turbulence. Burgers proposed the equation[1,2]

$$\frac{\partial}{\partial t}u(t,x)+u(t,x)\frac{\partial}{\partial x}u(t,x)=\nu\frac{\partial^2}{\partial x^2}u(t,x) \tag{1}$$

as a one-dimensional analogy of the Navier–Stokes equation in order to simplify the problem of turbulence by avoiding its complicated vectorial character.

At present we cannot numerically simulate the flow field at sufficiently high Reynolds number to produce the inertial-range in two- or three-dimensional flow because of insufficient computer capacity.[3–5] The one-dimensional model of turbulence is needed. The commonly used model is the Burgers equation (1) or its forced form, the so-called Burgers turbulence. The solutions of (1) can be expressed explicitly in terms of initial data and such a turbulence (without external force) has been studied by many authors.[6–11] The numerical experiments dealing with an external force were made by Jeng[12] for small viscosity and Kida and Sugihara[13] for the inviscid limit.

All the analytical and numerical studies lead to the conclusion that the k^{-2} inertial-range spectrum is the characteristic feature of the Burgers turbulence. In contrast, for the Navier-Stokes turbulence the cascade transfer of energy from large eddies to small eddies yields Kolmogorov's $k^{-5/3}$ inertial-range spectrum. That is related to the essential difference between the Burgers equation and the Navier–Stokes equation, and indicates that the Burgers equation is not a proper one-dimensional model of the Navier–Stokes turbulence.[14]

This paper consists of two parts. In the first part, the Burgers equation with a steady external force acting at the lowest wavenumber is numerically integrated in order to study the evolution of its solutions. The numerical results show that after a sufficiently long time these solutions reach a steady state of "laminar flow," which has no randomness and is independent of the initial conditions, i.e., absolutely stable to disturbances. The essential characteristics of a turbulence are its randomness and instability to small disturbances. Hence, strictly speaking, the so-called Burgers turbulence is not a turbulence.

In the second part of this paper, a new mathematical model is proposed as an one-dimensional analogy of the Navier–Stokes equation. It has a modified advection term and a pressure-type term. A series of numerical experiments on this one-dimensional model are made. We succeed in obtaining Kolmogorov's $k^{-5/3}$ inertial-range spectrum. The (one-dimensional) Kolmogorov constant ranges from 0.5 to 0.65.

Our numerical experiments confirm the vital role of the pressure term in hydrodynamic turbulence. The nonlinear interaction of the advection term alone cannot generate turbulence. The commonly used one-dimensional model of turbulence (the Burgers turbulence) has a k^{-2} inertial-range spectrum. We are successful in proposing a one-dimensional model of the Navier–Stokes turbulence, which has Kolmogorov's $k^{-5/3}$ inertial-range spectrum.

II. THE FORCED BURGERS EQUATION AND ITS FOURIER TRANSFORM

With a characteristic length L and a characteristic velocity V by means of the dimensionless quantities $x'=x/L$, $t'=tV/L$ and $\nu'=\nu/(VL)$, Eq. (1) becomes

$$\frac{\partial}{\partial t'}u'+u'\frac{\partial}{\partial x'}u'=\nu'\frac{\partial^2}{\partial x'^2}u'. \tag{2}$$

If we drop the primes in (2), (1) and (2) are identical. Hence (1) can be understood as the dimensionless form of the Burgers equation, and ν is the reciprocal of Reynolds number. Afterwards all quantities and equations are assumed to be dimensionless.

Assuming the periodic boundary condition

$$u(t,x+2\pi)=u(t,x), \tag{3}$$

we can expand $u(t,x)$ into the Fourier series

$$u(t,x)=\sum_k U(k)\exp(ikx), \tag{4}$$

where

[a)] Permanent address: P.O. Box 3928, Beijing, The People's Republic of China.

 0031-9171/84/081957-09$01.90

$$U(k)=\frac{1}{2\pi}\int_0^{2\pi} u(t,x)\exp(-ikx)\,dx \tag{5}$$

is a function of time t. From (4), the Burgers equation (1) becomes

$$\frac{d}{dt}U(k)=-ikW(k)-\nu k^2U(k), \tag{6}$$

and

$$W(k)=\frac{1}{2}\sum_p U(p)U(k-p) \tag{7}$$

by the convolution theorem.

If there is an external force, which is supposed to have the simple form $\mu(k)U(k)$, (6) can be generalized as follows

$$\frac{d}{dt}U(k)=-ikW(k)+\mu(k)U(k)-\nu(k)U(k). \tag{8}$$

Both $\mu(k)$ and $\nu(k)$ in (8) are positive, $\mu(k)U(k)$ corresponds to the energy source and $\nu(k)U(k)$ corresponds to the energy sink. When $\mu(k)=0$ and $\nu(k)=\nu k^2$, (8) becomes (6), and the energy sink is due to viscous dissipation.

The Fourier component $U(k=0)$ represents the mean flow of the velocity field. From (6), we see that the mode $k=0$ has no interaction with other modes. For simplicity, we assume that $U(k=0)=0$, i.e., there is no mean flow.

III. ENERGY EQUATION

The intensity of mode k is

$$e(k)=U(k)U^*(k). \tag{9}$$

The asterisk means complex conjugate. From (8) we have

$$\frac{d}{dt}e(k)=r(k)+2\mu(k)e(k)-2\nu(k)e(k), \tag{10}$$

here

$$r(k)=-ik[W(k)U^*(k)-W^*(k)U(k)]. \tag{11}$$

From (7) and (11), it is easy to prove that

$$\sum r(k)=0. \tag{12}$$

The total energy of all modes is

$$\sum_{k>0}e(k)=\frac{1}{2\pi}\int_0^{2\pi}\left(\frac{u^2(t,x)}{2}\right)dx. \tag{13}$$

The energy flow rate across the k space is

$$q(k)=\sum_{k'>k}r(k')=-\sum_{k'=1}^{k}r(k'). \tag{14}$$

In inertial-range $\mu(k)=\nu(k)=0$, from (10) and (14), we have $r(k)=0$ and $q(k)=$ constant for a steady state.

The ensemble average applied to (10) gives

$$\frac{d}{dt}E(k)=R(k)+2\mu(k)E(k)-2\nu(k)E(k), \tag{15}$$

here

$$E(k)=\langle e(k)\rangle \tag{16}$$

is the energy spectrum, and

$$R(k)=\langle r(k)\rangle \tag{17}$$

is the energy transfer spectrum function, $\langle\cdots\rangle$ means ensemble average. The energy transfer function is

$$Q(k)=\langle q(k)\rangle=\sum_{k'>k}R(k')=-\sum_{k'=1}^{k}R(k'). \tag{18}$$

In inertial-range $\mu(k)=\nu(k)=0$, from (15) and (18) we have $R(k)=0$ and

$$Q(k)=\epsilon(\text{constant}) \tag{19}$$

for a stationary turbulence. The ϵ is the energy dissipation rate.

IV. INERTIAL-RANGE DYNAMICS

The idealized model of inertial-range dynamics is that an energy source is at the lowest wavenumber and a sink is at infinite wavenumber, with an energy flow across the spectrum at a constant rate ϵ. It is impossible to work with infinite wavenumber in a numerical experiment. The truncation approximation must be used, i.e., assuming

$$U(k)=0,\quad \text{if } k>k_c. \tag{20a}$$

Here k_c is called the cutoff wavenumber. The energy source is supposed to be acting at the lowest wavenumber $k=1$ only, i.e.,

$$\mu(k)=0,\quad \text{if } k>1. \tag{20b}$$

The sink is acting over the neighborhood of the cutoff wavenumber k_c only, i.e.,

$$\nu(k)=0,\quad \text{if } k\leqslant k_d \tag{20c}$$

where k_d is less than k_c but near k_c.

By (20), the generalized Burgers equation (8) becomes

$$\frac{d}{dt}U(1)=-iW(1)+\mu(1)U(1), \tag{21a}$$

$$\frac{d}{dt}U(k)=-ikW(k),\quad \text{if } 2\leqslant k\leqslant k_d, \tag{21b}$$

$$\frac{d}{dt}U(k)=-ikW(k)-\nu(k)U(k),\quad \text{if } k_d<k\leqslant k_c. \tag{21c}$$

Equations (21) describe the following process: The energy is input at $k=1$, is transferred to high wavenumbers by the nonlinear interaction $W(k)$, and finally is dissipated over the neighborhood of k_c. With the truncation approximation (20a), after some manipulation, Eq. (7) becomes

$$W(k)=\sum_{p=1}^{k_c-k}U(-p)U(k+p)+\frac{1}{2}\sum_{p=1}^{k-1}U(p)U(k-p). \tag{22}$$

V. ENERGY SOURCE AND ENERGY SINK

Tentative numerical experiments of (21) show that when $\mu(1)$ in (21a) is too small the modal intensity $e(k)$ decreases with time; when $\mu(1)$ is too large the $e(k)$ increases with time, leading to overflow. It is more convenient to use a reservoir-type energy source which is able to adjust its input power automatically to keep the modal intensity $e(1)$ constant. There are many ways to construct such an energy source. One way to do it is to replace (21a) by

$$\frac{d}{dt}U(1)=-iW(1)+C[|U_0(1)|-|U(1)|]U(1). \tag{23}$$

Here C is a large positive amplification factor and $U_0(1)$ is the initial value of $U(1)$. The $|\cdots|$ means absolute value. The advection term $-iW(1)$ in (23) transfers the energy from mode 1 to other modes and reduces the intensity of mode 1; the energy source represented by the last term in (23) inputs energy to mode 1 as soon as its intensity becomes less than the initial value, similar to a simple feedback system. An ideal reservoir-type energy source can balance the advection term $-iW(1)$ exactly and keep $U(1)$ a constant, i.e.,

$$\frac{d}{dt}U(1)=0. \tag{24}$$

In our numerical experiments the $\nu(k)$ in (21c) assumes the following form

$$\nu(k)=\nu_d(k-k_d)^n. \tag{25}$$

Here ν_d and n are positive numbers. This structure of $\nu(k)$ makes the transition from the inertial range to the dissipation range a smooth one. Our numerical experiments show that the detailed structure of $\nu(k)$ does not influence the outcomes of the inertial-range dynamics, so long as the intensity of the energy sink matches the intensity of the energy source.

By (24) and (25), Eq. (21) becomes

$$\frac{d}{dt}U(1)=0 \quad \text{or} \quad U(1)=\text{const}, \tag{26a}$$

$$\frac{d}{dt}U(k)=-ikW(k), \quad \text{if } 2\leqslant k\leqslant k_d, \tag{26b}$$

$$\frac{d}{dt}U(k)=-ikW(k)-\nu_d(k-k_d)^nU(k),$$

$$\text{if } k_d<k\leqslant k_c. \tag{26c}$$

When k_c and k_d approach infinity, Eq. (26) corresponds to the inviscid limit of the Burgers equation with an energy source at $k=1$ and an energy sink at $k=\infty$.

The introduction of an energy source is indispensable for studying the long-time evolution of a turbulence. If there is no energy source, the turbulence will decay and finally die out due to dissipation.

VI. NUMERICAL EXPERIMENTS OF EQ. (26)

The Adams method is used to solve the initial-value problem of (26). The time increment $\Delta t=0.005$ for $k_c=50$ and $\Delta t=0.0025$ for $k_c=100$ in order for the numerical process to be stable. Ten runs of such numerical experiments of (26) have been made on computer corresponding to four different initial conditions, two cutoff wavenumbers and three types of energy sink. They are summed up in Table I and Figs. 1–4. The four initial conditions are

$$\begin{cases} U(1)=1, & \text{(27a)}\\ U(k)=0.3, \quad \text{if } 2\leqslant k\leqslant 5, & \text{(27b)}\\ U(k)=0.001, \quad \text{if } 6\leqslant k\leqslant k_c, & \text{(27c)}\end{cases}$$

$$\begin{cases} U(1)=1, & \text{(28a)}\\ U(k)=0.31623, \quad \text{if } 2\leqslant k\leqslant 5, & \text{(28b)}\\ U(k)=0.001, \quad \text{if } 6\leqslant k\leqslant k_c, & \text{(28c)}\end{cases}$$

$$\begin{cases} U(1)=1, & \text{(29a)}\\ U(k)=0.21, \quad \text{if } 2\leqslant k\leqslant 10, & \text{(29b)}\\ U(k)=0.001, \quad \text{if } 11\leqslant k\leqslant k_c, & \text{(29c)}\end{cases}$$

and

$$\begin{cases} U(1)=\exp(i\pi/2), & \text{(30a)}\\ U(k)=0.21\exp(i\pi k/2), \quad \text{if } 2\leqslant k\leqslant 10, & \text{(30b)}\\ U(k)=0.001\exp(i\pi k/2), \quad \text{if } 11\leqslant k\leqslant k_c. & \text{(30c)}\end{cases}$$

The general behavior of the solutions of (26) is illustrated in Fig. 1 which is the result of run 1 (the actual numerical computation was done up to time $t=15$ instead of $t=6$). Although Fig. 1 shows the time variation of the total energy only, the time variation of the intensity and the phase of each mode have the same behavior. During the early stage the solutions of (26) undergo a transient process, the intensity of each mode except mode 1 varies with time rapidly. This transient process begins at $t=0$ and ends at $t=4$. After $t=4$ the solutions of (26) reach a steady state of "laminar flow," which is characterized by the k^{-2} law for the modal intensity in the range $3<k<k_c/3$. (See Figs. 1–4.) It has to be emphasized that the numerical results given in Figs. 1–4 are for a single realization, no ensemble average or time average has been made.

In the final steady state of "laminar flow," the amplitude and phase of all modes are independent of time, so there is no randomness in the flow field at all. Moreover, the final steady state of "laminar flow" is independent of the initial conditions, hence it is absolutely stable to the disturbances. A comparison of Figs. 2 and 3 shows that in the final steady state of "laminar flow" the behavior of the inertial range $(3<k<k_c/3)$ is independent of the structure of the energy

TABLE I. Parameters for numerical experiments of Eq. (26) (Figs. 1–4).

Run No.	Initial condition	Cutoff wavenumber k_c	Energy sink ν_d	Energy sink n	Energy sink k_d	Time increment Δt
1	Eq. (27)	50	0.2	3	40	0.005
2	Eq. (28)	50	0.2	3	40	0.005
3	Eq. (29)	50	0.2	3	40	0.005
4	Eq. (30)	50	0.2	3	40	0.005
5	Eq. (27)	50	0.25	2	30	0.005
6	Eq. (29)	50	0.25	2	30	0.005
7	Eq. (27)	100	0.2	2	60	0.0025
8	Eq. (28)	100	0.2	2	60	0.0025
9	Eq. (29)	100	0.2	2	60	0.0025
10	Eq. (30)	100	0.2	2	60	0.0025

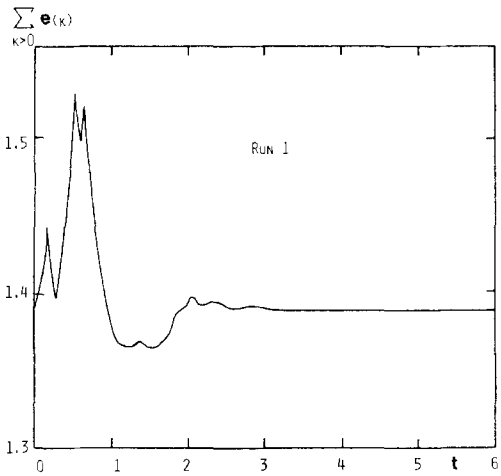

FIG. 1. Time variation of total energy.

sink, whose influence is limited to the neighborhood of the dissipation range.

In the runs 1–6, the cutoff wavenumber $k_c = 50$, in the runs 7–10 $k_c = 100$. The increase of the cutoff wavenumber k_c leads to the broadening of the inertial-range proportionally, but the behavior of the inertial-range remains the same, see Figs. 2–4. It is logical to conclude that the general characteristics of the solutions of Eq. (26) will remain the same when the cutoff wavenumber k_c approaches infinity and the inertial-range becomes infinitely wide, which corresponding to the inviscid limit of the Burgers turbulence with an energy source at $k = 1$ and an energy sink at $k = \infty$. If we consider an ensemble of many realizations, corresponding to different initial conditions and different external forces at lower wave-

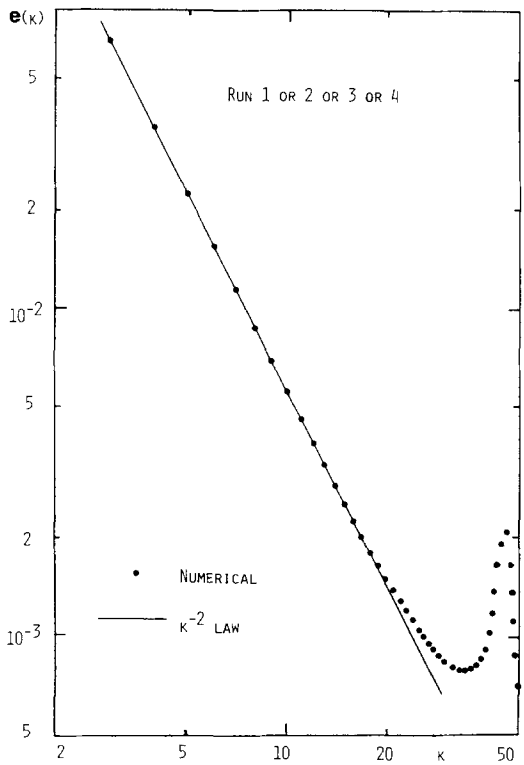

FIG. 2. Modal intensity of final steady state of "laminar flow."

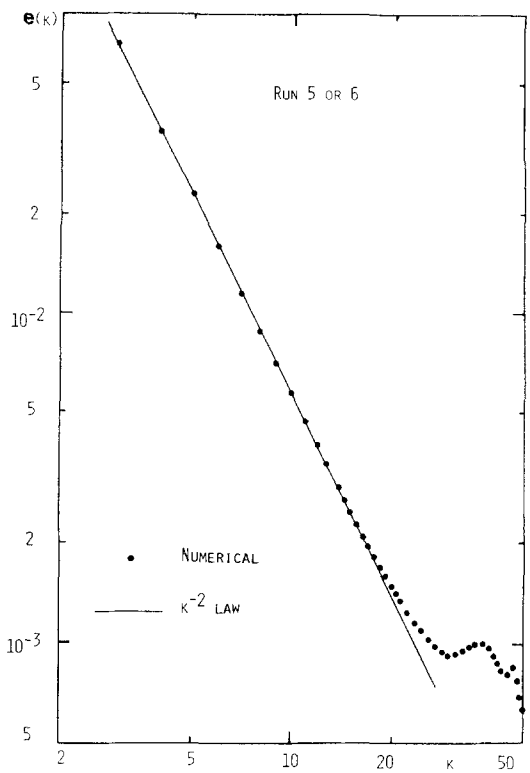

FIG. 3. Modal intensity of final steady state of "laminar flow."

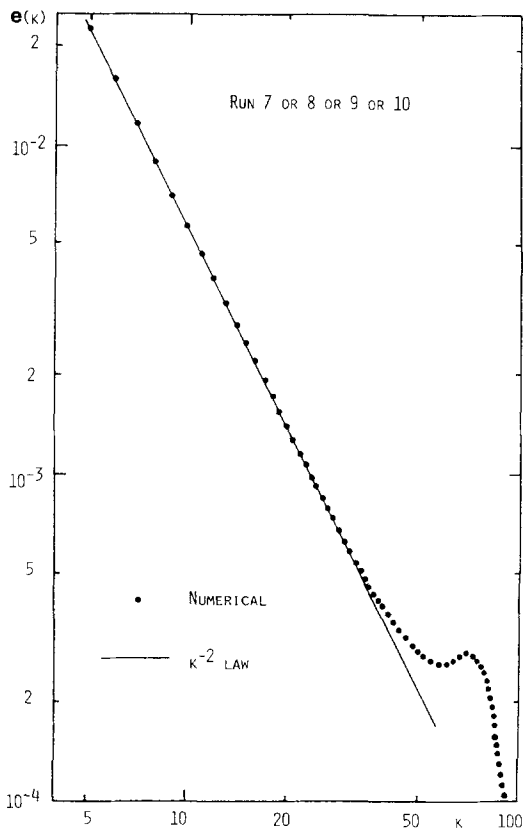

FIG. 4. Modal intensity of final steady state of "laminar flow."

numbers, the ensemble average will yield the well-known k^{-2} inertial-range spectrum, since the modal intensity of each realization is proportional to k^{-2} in the inertial range according to our numerical experiments.

VII. THE BURGERS TURBULENCE IS NOT A TURBULENCE

The essential characteristics of a turbulence is its apparent randomness and instability to small disturbances. Two turbulent flows that are nearly identical in detail will appear dramatically different at later time, i.e., the extreme sensitivity of the solution of the hydrodynamic equation to the initial conditions. In the Burgers equation the only nonlinear term is the advection term, there is no pressure term. According to our numerical experiments desribed in Sec. VI, the nonlinear interaction of the advection term reduces the chaos of the flow field and builds up correlation between modes, finally leads to a steady state of "laminar flow" which is stable to disturbances. The advection term alone cannot generate turbulence, no matter how high the Reynolds number. Hence, strictly speaking, the so-called Burgers turbulence is not a turbulence.

In the Navier–Stokes turbulence the pressure term plays the role of a high-frequency random force to limit the buildup of correlation between modes, the vortex structure in the flow field is not stable. The chaos of the flow field increases with time, finally leading to a state of turbulence which is random and unstable to small disturbances.

The essential differences between the Burgers equation and the Navier–Stokes equation lead to different inertial-range spectrums: k^{-2} for the Burgers turbulence; and $k^{-5/3}$ for the Navier–Stokes turbulence. The Burgers equation is not a proper one-dimensional model of the Navier–Stokes turbulence. It is significant to have a one-dimensional model which can simulate the Navier–Stokes equation as well as possible and has Kolmogorov's $k^{-5/3}$ inertial-range spectrum. The numerical experiments on this one-dimensional model can be used to test various theories of turbulence.

VIII. ONE-DIMENSIONAL MODEL OF NAVIER–STOKES TURBULENCE

The proposed one-dimensional model has the following form:

$$\frac{d}{dt}U(k) = -ikW_m(k) + P(k) - \nu(k)U(k). \tag{31}$$

Here the $-ikW_m(k)$ is a modified advection term, which transfers the energy from one mode to the others but conserves the total energy of all modes. The $P(k)$ is a pressure-type term to simulate the role of the pressure term of the Navier–Stokes equation as a high-frequency conservative random force.

The Navier–Stokes equation can be transformed into the following form[15–17]

$$\frac{d}{dt}X_i = -\nu_i X_i + \sum_{j,m} A_{ijm}X_jX_m. \tag{32}$$

Here the $(X_i;\ i\geqslant 0)$ is the complete set of independent real modal parameters, and is related to the real and imaginary parts of the complex Fourier components of the turbulent velocity field. The remarkable property of the nonlinear interaction coefficients A_{ijm} is that[15]

$$A_{ijm} = 0,$$

if any two of i,j,m are equal. (33)

The property (33) is related to the incompressibility which requires the Fourier components of the velocity field to be perpendicular to its wavenumber vector. However, when we transform the Burgers equation (6) into the form (32), the corresponding nonlinear interaction coefficients will not satisfy (33), for no incompressibility condition. In order for the one-dimensional model (31) to simulate the Navier–Stokes equation as well as possible, the $W_m(k)$ in (31) is defined as follows

$$W_m(k) = W(k) - iU^{(2)}(2k)U^*(k), \quad \text{if } k \text{ is odd;} \tag{34a}$$

$$W_m(k) = W(k) - iU^{(2)}(2k)U^*(k) - 0.5[U^{(1)}(k/2)]^2 + 0.5[U^{(2)}(k/2)]^2, \quad \text{if } k \text{ is even.} \tag{34b}$$

Here $W(k)$ is given by (7), the $U^{(1)}(k)$ and $U^{(2)}(k)$ are the real and imaginary parts of $U(k)$, respectively. We obtain (34) simply by discarding these terms in $W(k)$ which will not satisfy (33).

Similar to (10), the energy equation of the one-dimensional model (31) is

$$\frac{d}{dt}e(k) = r_m(k) + U^*(k)P(k) + U(k)P^*(k) - 2\nu(k)e(k), \tag{35}$$

here

$$r_m(k) = -ik[W_m(k)U^*(k) - W_m^*(k)U(k)]. \tag{36}$$

From (34) and (36), we have

$$\sum r_m(k) = 0. \tag{37}$$

Equation (37) means that the nonlinear term $-ikW_m(k)$ of (31) conserves the total energy of all modes.

The pressure term in the Navier–Stokes equation likes a special "isotropic" conservative force; it scarcely transfers the energy from lower wavenumbers to higher wavenumbers, but tends to equipartition the energy among all degrees of freedom of the same wavenumber. In the one-dimensional case, there are only two degrees of freedom for the same wavenumber, corresponding to the real and imaginary parts of $U(k)$, respectively. In order for the term $P(k)$ in (31) to simulate the pressure term of the Navier–Stokes equation as an "isotropic" conservative force, it is required that

$$U^*(k)P(k) + U(k)P^*(k) = 0. \tag{38}$$

Let $\phi(k)$ be the phase of mode k, i.e.,

$$\exp[i\phi(k)] = U(k)/|U(k)|, \tag{39}$$

then (38) means that

$$P(k) = \pm i|P(k)|\exp[i\phi(k)]. \tag{40}$$

If the intensity of all modes is amplified by the same factor C, the pressure term in the Navier–Stokes equation will be amplified by the same factor C too. Therefore we choose

$$P(k) = iA(k)|U(1)|^2\exp[i\phi(k)]. \tag{41}$$

Here $A(k)$ is real, positive or negative. The pressure term in the Navier–Stokes turbulence plays the role of a random force to limit the buildup of correlation between modes, hence, we simply let $A(k)$ to be random variables.

In numerical experiments the $A(k)$ is simulated by the uniformly distributed pseudorandom numbers over the interval $(-a,a)$, based on the recurrent use of residues,[18]

$$\alpha_{n+1} = \beta\alpha_n (\text{mod } M). \tag{42}$$

For example $\beta = 7^9$ and $M = 10^{10}$. In our most numerical experiments, $a = 2$, so the average amplitude of $A(k)$ is equal to 1. The structure of $A(k)$ will be described in detail later.

It has to be pointed out that the above reasoning and argument leading to the one-dimensional mode (31) with (34) and (41) is plausible and rather arbitrary. The final justification of this mathematical mode is that it is able to simulate the essential characteristics of the Navier–Stokes turbulence and yields the Kolmogorov's $k^{-5/3}$ inertial-range spectrum. We are not going to transform (31) into (t,x) space and give the resulting equation a specious "physical meaning." We prefer to work in the (t,k) space and consider our model (31) merely a mathematical model of turbulence.

IX. ENSEMBLE AVERAGE AND TIME AVERAGE

According to Secs. IV and V, for studying the inertial-range dynamics, Eq. (31) becomes

$$\frac{d}{dt}U(1) = i\omega U(1), \tag{43a}$$

$$\frac{d}{dt}U(k) = -ikW_m(k) + P(k), \quad 2 \leqslant k \leqslant k_d, \tag{43b}$$

$$\frac{d}{dt}U(k) = -ikW_m(k) + P(k) - \nu_d(k-k_d)^n U(k), \quad k_d < k \leqslant k_c. \tag{43c}$$

If $\omega = 0$, (43a) is the same as (26a), then the energy source is identical with that described in the Sec. V. The introduction of ω in (43a) is for the convenience of numerical computation. The energy transfer rate from mode 1 to mode 2, from mode 2 to mode 4, and so on, is quite sensitive to the phase of mode 1. In order to calculate the spectrum and other statistical properties of a turbulence by ensemble average, it is necessary to take account of all possible phases of mode 1. When using (26a) instead of (43a), we have to solve the initial-value problem of (43) for many different initial phases of mode 1. It will require much computing time. When (43a) is used with a proper vale of ω, the phase of mode 1 is rotating with angular velocity ω; it is possible to use the time average over a finite period to replace the ensemble average and save much computing time.

The stationarity of the turbulence is another reason why we can use the time average to replace the ensemble average. The energy source at mode 1 is continuously supplying the energy to the turbulence to prevent it from decaying. After the early transient process ended, the solutions of (43) can be considered a stationary stochastic process, the time average is equal to the ensemble average. In our numerical experiments the time average is taken over the interval from $t = 10$ to $t = 60$ or 110. The numerical results show that the initial conditions have little influence on the outcomes of the time-averaging of the solutions of (43), thereby confirm the legality of using the time average.

The energy spectrum $E(k)$, the energy transfer spectrum function $R(k)$, and the energy transfer function $Q(k)$ are given by (16)–(19), but the $r(k)$ in (17) has to be replaced by $r_m(k)$ of (36), and the ensemble average is replaced by the time average in the numerical experiments.

X. NUMERICAL EXPERIMENTS OF EQ. (43)

The Adams method is used to solve the initial-value problem of (43) up to $t = 60$ or 110, then the time average from $t = 10$ to $t = 60$ or 110 is used to calculate the energy spectrum $E(k)$ and the energy dissipation rate ϵ. The cutoff wavenumber $k_c = 50$ or 80. The time increment $\Delta t = 0.005$ for $k_c = 50$, and $\Delta t = 0.01/3$ for $k_c = 80$, in order for the numerical process to be stable.

The random variable $A(k)$ in (41) is constructed by the following procedure. First (42) is used to produce 5000 random numbers $f(j)$ uniformly distributed over the interval $(-a,a)$,

$$-a \leqslant f(j) \leqslant a \quad (j = 1,2,...,5000). \tag{44}$$

Then for time $t = n\Delta T$ $(n = 0,1,2,...)$ the computer generates $(k_c - 1)$ pseudorandom integer numbers $s(k,n)$ $(k = 2,3,...,k_c)$ which can be any integer between 1 and 5000, by means of (42). The ΔT will be defined later. Finally, let

$$A(k) = f[s(k,n)] \quad \text{for} \quad n\Delta T \leqslant t < (n+1)\Delta T. \tag{45}$$

The average amplitude of $A(k)$ is $a/2$. The ΔT can be roughly considered the correlation time of the random processes $A(k)$. In order for $P(k)$ to simulate the pressure term of the Navier–Stokes turbulence as a high-frequency random force, we must let

$$\Delta T \ll 1. \tag{46}$$

In order for the Adams method to be suitable for solving (43) which has a rapidly fluctuating term $P(k)$, we must let

$$\Delta T \gg \Delta t. \tag{47}$$

In the numerical experiments we choose $\Delta T = 10\Delta t$. For example, for $k_c = 50$, $\Delta t = 0.005$, so $\Delta T = 0.05$ which satisfies both (46) and (47).

More than ten runs of the numerical experiments of (43) have been made on computer, corresponding to different initial conditions, different cutoff wavenumbers, different sets of random numbers for $A(k)$, different sources and different sinks. We succeed in obtaining the Kolmogorov law for the inertial-range spectrum:

$$E(k) = \text{Ko}\,\epsilon^{2/3} k^{-5/3}. \tag{48}$$

The dimensionless constant Ko is still called the (one-dimensional) Kolmogorov constant. The numerical results of four of these runs and the relevant parameters are given in Figs. 5–8 and Table II.

The initial conditions and the structure of the energy sink have little influence on the inertial-range spectrum. The influence of the energy sink is limited to the neighborhood of the dissipation range. When the cutoff wavenumber increases from 50 to 80, the inertial-range $3 < k < k_c/4$ be-

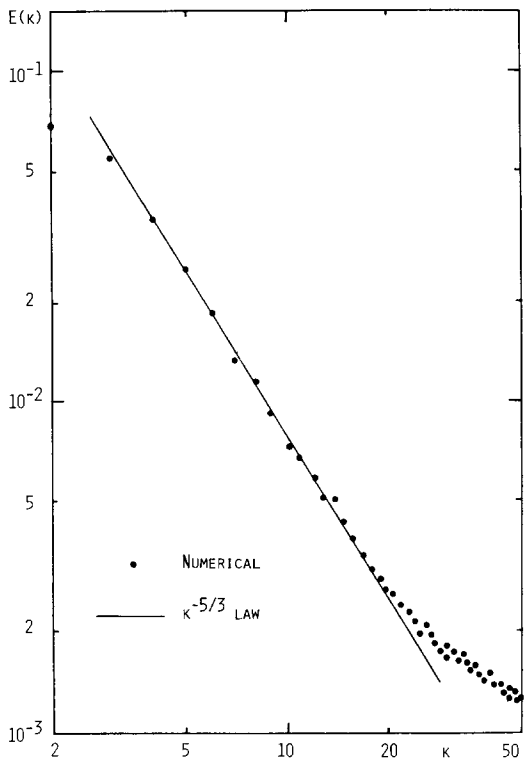

FIG. 5. Energy spectrum of one-dimensional turbulence.

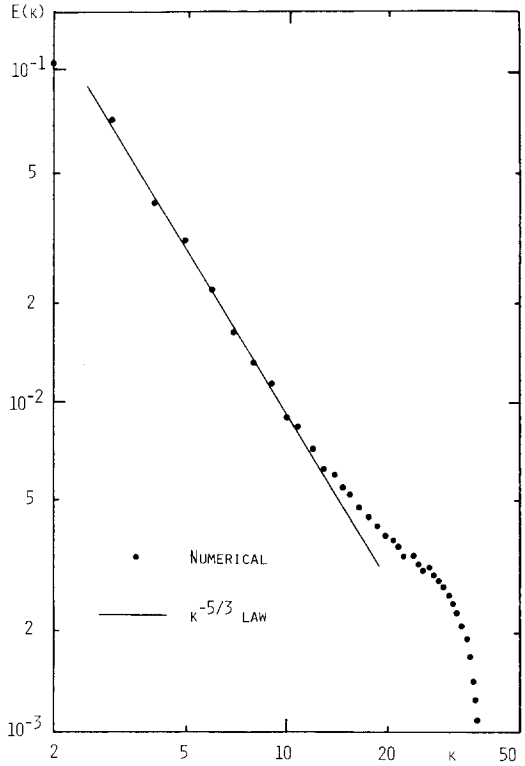

FIG. 7. Energy spectrum of one-dimensional turbulence.

comes wider proportionally, and the Kolmogorov constant seems to decrease slightly. See Figs. 5–7.

The average amplitude $a/2$ of $A(k)$ has great influence on the spectrum. When a is very small, the term $P(k)$ can be neglected and (31) becomes a modified Burgers equation, we get k^{-2} inertial-range spectrum. When a is very large, the term $P(k)$ will be dominant and the advection term can be omitted, the inertial-range spectrum is neither k^{-2} nor $k^{-5/3}$ type. When $1 \leqslant a \leqslant 3$, i.e., the average amplitude is between 0.5 and 1.5, both the modified advection term and the pres-

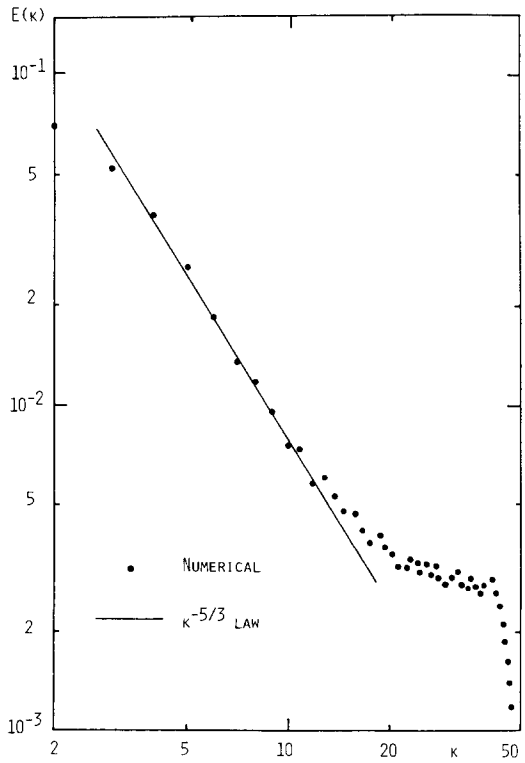

FIG. 6. Energy spectrum of one-dimensional turbulence.

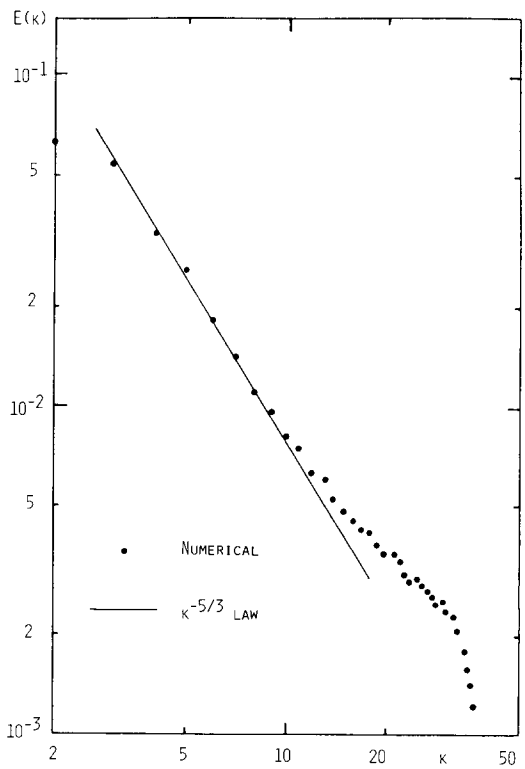

FIG. 8. Energy spectrum of one-dimensional turbulence.

TABLE II. Parameters for numerical experiments of Eq. (43) (Figs. 5–8).

Fig. No.	Initial condition	Cutoff wavenumber k_c	Energy source ω	Energy sink ν_d	n	k_d	Interval for time-averaging	Dissipation rate of energy ϵ	Kolmogorov constant Ko
5	Eq. (28)	80	$\pi/2$	0.2	2	50	10– 60	0.470	0.60
6	Eq. (28)	50	$\pi/2$	0.1	3	40	10– 60	0.451	0.63
7	Eq. (28)	50	1	0.2	2	30	10–110	0.645	0.58
8	Eq. (49)	50	0	0.2	2	30	10– 60	0.457	0.61
			[the average amplitude of $A(k)$ is $a/2 = 1$ for Figs. 5–8]						

sure-type term are important in (31) or (43), similar to the case of the Navier–Stokes equation, and we obtain the Kolmogorov's $k^{-5/3}$ inertial-range spectrum (48). The Kolmogorov constant increases by 10%–20% as the average amplitude of $A(k)$ increases from 0.5 to 1.5. If different values of α_0, β, and M in (42) are used, different sets of $f(j)$ and $A(k)$ can be obtained by means of (44) and (45). When using different sets of $A(k)$, we still get the Kolmogorov inertial-range spectrum (48) with slightly different Kolmogorov constant, so long as the average amplitude of $A(k)$ is the same and between 0.5 and 1.5. Figures 5–8 correspond to $a = 2$.

The introduction of the angular velocity ω in (43a) enables us to use the time average over a finite period to replace the ensemble average to calculate the spectrum $E(k)$ and the energy dissipation rate ϵ, but the value of ω cannot be too large. When ω is greater than three in the case of the modal intensity $e(1) = 1$, the inertial-range spectrum begins to be different from the Kolmogorov inertial-range spectrum (48). When ω increases from 1 to $\pi/2$, the Kolmogorov constant increases a little, see Figs. 6 and 7.

As mentioned in the preceding section, when $\omega = 0$ the energy flow rate from mode 1 to higher modes strongly depends on the phase of mode 1. If the phase of model 1 is 0, the energy flow rate is nearly zero; if the phase of mode 1 is $\pi/4$, the energy flow rate is maximum; if the phase of mode 1 is $\pi/6$, the energy flow rate is medial. Hence, we expect that when $\omega = 0$ and the phase of mode 1 is $\pi/6$, the time average over a finite period will also correspond to the ensemble average. In order to confirm this expectation, we use the following initial condition

$$\begin{cases} U(1) = \exp(i\pi/6), & \text{(49a)} \\ U(k) = 0.31623, \quad \text{if } 2 \leqslant k \leqslant 5, & \text{(49b)} \\ U(k) = 0.001, \quad \text{if } 6 \leqslant k \leqslant k_c & \text{(49c)} \end{cases}$$

and let $\omega = 0$ in (43a), then do the numerical experiment of (43). Its result is shown in Fig. 8, which confirms the expectation.

The (one-dimensional) Kolmogorov constant obtained in our numerical experiments of (43) ranges from 0.5 to 0.65. Ko = 0.5 is obtained in the case of $\omega = 1$, $k_c = 80$, and $a = 1$. Ko = 0.65 is obtained in the case of $\omega = \pi/2$, $k_c = 50$, and $a = 3$.

The outcome of the time-averaging over longer time interval is more smooth and has less fluctuation. Figure 7 shows the result of the time average from $t = 10$ to $t = 110$. Figures 5, 6, and 8 show the results of the time average from $t = 10$ to $t = 60$.

XI. DISCUSSION

The argument, which leads Kolmogorov to propose the $k^{-5/3}$ law for the inertial-range spectrum of a turbulence,[19,20] is so general that it is logical to expect that Kolmogorov's $k^{-5/3}$ law is valid despite the dimensionality of a turbulence. Unfortunately the commonly used one-dimensional model of turbulence (the Burgers turbulence) has the k^{-2} inertial-range spectrum instead of $k^{-5/3}$. Hence two questions arise. The first one is: what is the essential difference between the Burgers equation and the Navier–Stokes equation which leads to the different inertial-range spectrums? The second question (which is more challenging) is: how does one find a proper one-dimensional model of turbulence which has Kolmogorov's $k^{-5/3}$ inertial-range spectrum? We hope this paper can help to answer the two questions.

The numerical experiments reported in this paper confirm the vital role of the pressure term in the hydrodynamic turbulence. The advection term builds up the correlation between modes and reduces the chaos of the flow field; finally, all modes are precisely locked in phase over the entire spectrum. The nonlinear interaction of the advection term alone cannot generate turbulence. The pressure term acts as a high-frequency conservative random force to limit the buildup of correlation between modes and to destroy the spectrum-wide phase locking, leading to a turbulence with Kolmogorov's $k^{-5/3}$ spectrum for the inertial subrange.

Tatsumi and Kida[10,11] treat the Burgers turbulence with the statistics of shock waves. In their treatment the velocity field $u(t,x)$ is determined by the initial condition $u(0,x)$ in a deterministic way, the randomness of the turbulence artificially comes into the flow field through the initial ensemble, instead of being generated by the Burgers equation itself. The velocity field of a single realization is not a stochastic process. They obtain the k^{-2} inertial-range spectrum, by assuming that the correlation of velocity field approaches zero faster than any negative power of r as r approaches infinity. Actually the k^{-2} inertial-range spectrum, according to our numerical experiments of Eq. (26), is merely a simple consequence of the fact that the modal intensity of the inertial-range of each realization is proportional to k^{-2} after the transient process ended. Since the modal intensity of each realization is proportional to k^{-2}, no matter what the initial condition is, an asymptotic k^{-2} inertial-range spectrum is evidently valid for any ensemble of initial velocity field.

In Jeng's and Kida-Sugihara's numerical experiments

of forced Burgers turbulence,[12,13] they also get k^{-2} inertial-range spectrum, and the randomness of the turbulent field is produced by the random external force acting at lower wavenumbers in addition to a random initial velocity distribution. In the Navier–Stokes turbulence the randomness and instability to disturbances are inherent properties of the Navier–Stokes equation. The external force is sometimes introduced to prevent the turbulence from decaying so that we can deal with a stationary turbulence.[15,16]

In our opinion, the difference between the Burgers equation and the Navier–Stokes equation is more interesting than their similarities. It is significant to have a one-dimensional model of the Navier–Stokes turbulence, which yields Kolmogorov's $k^{-5/3}$ inertial-range spectrum. In this paper we propose such a one-dimensional model. According to the numerical experiments of Eq. (43), the Kolmogorov constant of this one-dimensional turbulence is between 0.5 and 0.65. This result can be used to test various approaches to the closure problems of turbulence theory.

Our numerical experiments are over a wavenumber range of 50–100. Of course nowadays computers allow us to do numerical study of the (three-dimensional) Navier–Stokes equation over a wavenumber range of almost the same order and a numerical study of the Burgers equation over a wavenumber range of thousands. But the numerical study of the Navier–Stokes equation over wavenumber range of the same order (e.g., 32) could hardly provide any significant information on the inertial-range dynamics of a turbulence. For our numerical experiments the wavenumber range of 50–100 is wide enough to produce an inertial subrange containing enough experimental data to indicate whether the specturm is k^{-2} or $k^{-5/3}$, and in the case of $k^{-5/3}$, to obtain quite accurate Kolmogorov constant. In the numerical experiments of Eq. (26) the emphasis is on the study of long-time evolution of a single realization. In the numerical experiments of (43) the emphasis is on the time-averaging over a long period to get a $k^{-5/3}$ inertial-range spectrum and the Kolmogorov constant.

Introducing an energy source at the lowest wavenumber is fruitful. If there is no energy source, due to dissipation, a turbulence will decay and finally die out; there is no possibility to study the long-time evolution of a single realization. Moreover, in the numerical experiments of Eq. (43) the solution of (43) becomes a stationary stochastic process due to the balance between the energy source and sink. Therefore it is possible to use the time average to replace ensemble average and save much computing time.

It is advisable to consider the one-dimensional model (31) or (43) as a purely mathematical model of hydrodynamic turbulence. It is not recommended to transform the one-dimensional model (31) into (t,x) space and to extract the "physical meaning" of the resultant equation. The most important thing is that the model (31) or (43) can simulate the essential feature of the cascade transfer of energy in a turbulence and has a Kolmogorov $k^{-5/3}$ inertial-range spectrum.

ACKNOWLEDGMENTS

The author would like to express his appreciation to Professor C. M. Tchen of the City College of New York for his guidance and encouragement. Also the author is grateful to the computer center of CUNY for the use of the computer.

[1] J. M. Burgers, Adv. App. Mech. **1**, 171 (1948).
[2] J. M. Burgers, *The Non-linear Diffusion Equation* (Reidel, Hingham, MA, 1974).
[3] S. A. Orszag and G. S. Patterson, Phys. Rev. Lett. **28**, 76 (1972).
[4] J. R. Herring, S. A. Orszag, R. H. Kraichnan, and D. G. Fox, J. Fluid Mech. **66**, 417 (1974).
[5] B. Fornberg, J. Comput. Phys. **25**, 1 (1977).
[6] E. Hopf, Commun. Pure. Appl. Math. **3**, 20 (1950).
[7] J. D. Cole, Q. Appl. Math. **9**, 1225 (1951).
[8] D. T. Jeng, R. Foerster, S. Haaland, and W. C. Meecham, Phys. Fluids **9**, 2114 (1966).
[9] I. Hosokawa and K. Yamamto, Phys. Fluids **7**, 1683 (1970).
[10] T. Tatsumi and S. Kida, J. Fluid Mech. **55**, 659 (1972).
[11] S. Kida, J. Fluid Mech. **93**, 337 (1979).
[12] D. T. Jeng, Phys. Fluids **12**, 2006 (1969).
[13] S. Kida and M. Sugihara, J. Phys. Soc. Jpn. **50**, 1785 (1981).
[14] R. H. Kraichnan, Phys Fluids **11**, 265 (1968).
[15] J. Qian, Phys. Fluids **26**, 2098 (1983).
[16] J. R. Herring, Phys. Fluids **8**, 2219 (1965).
[17] D. C. Leslie, *Developments in the Theory of Turbulence* (Clarendon, Oxford, 1973).
[18] YU. A. Shreider, *Method of Statistical Testing* (Elsevier, New York, 1964).
[19] A. N. Kolmogorov, C. R. Acad.Sci. USSR **30**, 301 (1941).
[20] J. O. Hinze, *Turbulence*, 2nd ed. (McGraw-Hill, New York, 1975).